

# Microscopic study of energy and centrality dependence of transverse collective flow in heavy-ion collisions

L.V. Bravina,<sup>1,2</sup> Amand Faessler,<sup>1</sup> C. Fuchs,<sup>1</sup> and E.E. Zabrodin<sup>1,2</sup>

<sup>1</sup> *Institute for Theoretical Physics, University of Tübingen,  
Auf der Morgenstelle 14, D-72076 Tübingen, Germany*

<sup>2</sup> *Institute for Nuclear Physics, Moscow State University, 119899 Moscow, Russia*

## Abstract

The centrality dependence of directed and elliptic flow in light and heavy systems of colliding nuclei is studied within two microscopic transport models at energies from  $1A$  GeV to  $160A$  GeV. The pion directed flow has negative slope in the midrapidity range irrespective of bombarding energy and mass number of the colliding ions. In contrast, the directed flow of nucleons vanishes and even develops antiflow in the midrapidity range in (semi)peripheral collisions at energies around  $11.6A$  GeV and higher. The origin of the disappearance of flow is linked to nuclear shadowing. Since the effect is stronger for a light system, it can be distinguished from the similar phenomenon caused by the quark-gluon plasma formation. In the latter case the disappearance of the flow due to the softening of the equation of state should be most pronounced in collisions of heavy ions. The centrality dependence of the elliptic flow shows that the maximum in the  $\langle v_2(b) \rangle$  distribution is shifted to very peripheral events with rising incident energy, in accord with experimental data. This is an indication of the transition from baryonic to mesonic degrees of freedom in hot hadronic matter.

PACS numbers: 25.75.-q, 25.75.Ld, 24.10.Lx

## I. INTRODUCTION

Collective effects, such as the expansion of highly compressed nuclear matter in the direction perpendicular to the beam axis of colliding heavy ions at relativistic energies, are very important for the study of the nuclear equation of state (EOS) and for the search of a predicted transition to the a phase of matter, quark-gluon plasma (QGP). At present the transverse flow of particles is believed to be one of the most clear signals to detect the creation of the QGP in heavy-ion experiments (for recent review, see [1,2]). This explains the great interest of both experimentalists and theoreticians in the transverse flow phenomenon (see, e.g., [3–5] and references therein), which was predicted about 25 years ago [6] in nuclear shock wave model analysis.

Initially, the collective flow has been conventionally subdivided into the radial flow, which is azimuthally symmetric, the bounce-off or directed flow [7] in the reaction plane along the impact parameter axis ( $x$ -axis), and the squeeze-out flow developing out of the reaction plane. The latter two components represent the anisotropic part of the transverse flow and appear only in noncentral heavy-ion collisions. The first observation of the transverse flow was made by the Plastic Ball [8] and the Streamer Chamber [9] collaborations at the BEVALAC energies ( $E_{lab} = 100A$  MeV -  $1.8A$  GeV). Later on the directed flow of charged particles has been detected by E877 collaboration at the AGS energies ( $E_{lab} = 10.7A$  GeV) and by NA49 [10] and WA98 [11] collaborations at the SPS energies ( $E_{lab} = 158 A$  GeV).

The collective flow is a very suitable observable to characterise the reaction dynamics because it is extremely sensitive to the interactions between the particles. At intermediate (SIS) energies the evolution of flow is mainly governed by the density and momentum dependence of the long-range attractive and short-range repulsive nuclear forces in the medium, i.e., the nuclear mean field [12–14]. With rising energy (AGS, SPS) the mean field gets less important while new degrees of freedom, strings, come into play. It has been shown also that the transverse flow could carry the primary information about the softening of the EOS due to the QGP creation [15–17], including the subsequent hadronization, as well as the relaxation of the excited matter to (local) thermal equilibrium.

The advanced technique for the analysis of the flow at high energies, based on the Fourier expansion of the particle azimuthal distribution, has been developed in Refs. [18–20]. The distribution of the particles in the azimuthal plane can be presented as

$$\frac{dN}{d\phi} = a_0 \left[ 1 + 2 \sum_{n=1}^{\infty} v_n \cos(n\phi) \right], \quad (1)$$

where  $\phi$  is the azimuthal angle between the momentum of the particle and the reaction plane. The first two coefficients,  $v_1$  and  $v_2$ , are the amplitudes of the first and second harmonics in the Fourier expansion of the azimuthal distribution, respectively. The asymmetric fraction of the collective flow is decomposed in this analysis into the directed (bounce-off) flow of particles emitted preferentially along the  $x$ -axis, and the elliptic component, which is developed mostly either along the  $x$ -axis or in the squeeze-out direction. The coefficient  $v_2$ , therefore, characterises the eccentricity of the flow ellipsoid [18].

The importance of the elliptic flow to study collective effects in heavy-ion collisions was first stressed in [21]. In this paper the rotation of the elliptic flow from the squeeze-out direction to the bounce-off direction with rising projectile energy was discussed as well.

The alignment of the elliptic flow in the plane of the directed flow has been experimentally detected in Au+Au collisions at the AGS energies [22] and in Pb+Pb collisions at the SPS energies [10,23]. In [24] the sensitivity of the elliptic flow to the early pressure was noticed. The elliptic flow seems to be generated only during the very beginning of the collective expansion [24,25], while the radial flow is developing almost until the freeze-out. It was also pointed out that the elliptic flow should have a kinky structure [26] if the expanding and cooling fireball undergoes a first-order phase transition from the QGP to hadrons. Therefore, the characteristic features of the plasma hadronization can be traced by the dependence of the elliptic flow on the impact parameter [27].

Although the collective flow is a unique complex phenomenon, the variety of its signals is very rich. Lacking a first principles theoretical description of heavy-ion collisions, one definitely needs to explore semi-phenomenological models whose numerical predictions can be compared with the experimental data on nuclear collective effects in a wide energy range. These models can be classified in general either as macroscopic models or as microscopic ones. Macroscopic models are based on the hypothesis of (local) thermal equilibrium in the system achieved by the large number of various inelastic and elastic processes in the course of a nuclear collision. The many-body distribution functions, which characterise the nonequilibrium states, are rapidly reduced to the one-particle distribution functions (one for each particle species), and the kinetic stage emerges. At a longer time scale the system can reach the hydrodynamic stage, where its evolution is described in terms of the moments of the one-particle distribution functions, such as average velocities, energies, and number of particles. The evolution of a relativistic perfect fluid obeys the conservation of energy and momentum [28]

$$\partial_\mu T^{\mu\nu} = 0, \quad (2)$$

where

$$T^{\mu\nu} = (\varepsilon + P)u^\mu u^\nu + P g^{\mu\nu} \quad (3)$$

is the energy-momentum tensor, and  $\varepsilon$ ,  $P$ ,  $u^\mu$  are the energy density, pressure, and local four-velocity, respectively.

Without the EOS, which links the pressure  $P$  to the energy density  $\varepsilon$ , the system of hydrodynamic equations (2) - (3) is incomplete. Usually, the EOS is taken in a form

$$P = a\varepsilon \equiv c_s^2 \varepsilon, \quad (4)$$

with  $c_s$  being the speed of sound in the medium. Inserting different equations of state, particularly with and without the plasma EOS, into the one-, two-, or three-fluid hydrodynamic model [29–32] one can study the properties of the particle collective flow at various incident energies [15–17,21].

The microscopic models, developed to describe heavy-ion collisions in a wide range of bombarding energies, e.g. [33–41] and others, do not rely on the assumption of thermal equilibrium. They employ a dynamical picture of heavy-ion interactions, in which the parton-, string-, and transport approaches can be relevant. Though these models do not explicitly assume the formation of the QGP, the creation of the field of strongly interacted coloured

strings may be considered as a precursor of the quark-gluon plasma. Because of the uncertainties in the description of the early stage of heavy-ion collisions at ultrarelativistic energies, the microscopic and macroscopic models can be merged to implement the phase transition to the deconfined phase directly in the microscopic model [26,42,43].

In the present paper two microscopic models, QMD and QGSM, are employed to study the anisotropic flow components in collisions of light and heavy ions at energies from SIS to SPS. The main goal is to understand to what extent the characteristic signals of the hot nuclear matter can be reproduced without invoking the assumption of QGP creation. In other words, if the experimental data will noticeably diverge from the results of simulations, this can be considered as an indication on new processes not included into the models. The paper is organised as follows. A brief description of the models is given in Sec. II. Sections III and IV present the mass and impact parameter dependence of the simulated directed and elliptic flow,  $v_1$  and  $v_2$ , at SIS, AGS, and SPS energies. Results obtained are discussed in Sec. V. Finally, conclusions are drawn in Sec. VI.

## II. MODELS

The dynamics of nucleus-nucleus collisions at energies up to  $\sqrt{s} \approx 2A$  GeV per nucleon can be described in terms of reactions between hadrons and their excited states, resonances. At higher energies additional degrees of freedom, i.e. strings, should be taken into account to describe correctly the processes of multiparticle production. Therefore, we employ the quantum molecular dynamics (QMD) model [12,44] at the SIS energies, while at the AGS and SPS energies the quark-gluon string model (QGSM) [36] is applied.

In the QMD approach the particles are propagated according to Hamilton equations of motion until their mutual interactions. Each nucleon is represented by a Gaussian-shaped density in the phase space. The black disk approximation is used to determine the binary collision of hadrons. It implies that two hadrons can collide if the centroids of two Gaussians are closer than the distance  $d_0 = \sqrt{\sigma_{\text{tot}}(\sqrt{s})/\pi}$  during their propagation. The Pauli principle is taken into account by blocking the collision if the final states are already occupied in the phase space by other particles. Among the inelastic channels the  $\Delta(1232)$  resonance is the dominant one. Pion production takes place via resonance decay of  $\Delta(1232)$  and  $N^*(1440)$ . Pions, which can propagate freely, i.e. without any mean field, undergo, however, a complex chain of reabsorption and subsequent resonance decay processes before their freeze-out [45]. At SIS energies the reaction dynamics is governed by the interplay between the nuclear mean field and binary collisions, which play a minor role at low energies ( $100A$  MeV) due to the Pauli-blocking of possible scattering states, but become more and more important with rising incident energy. In the present work we employ Skyrme-type mean field with a density dependence corresponding to a hard EOS ( $K = 380$  MeV) and momentum dependence fitted to the empirical nucleon-nucleus optical potential [12]. This type of interaction has been shown to give a good description of flow data in the considered energy range around  $1A$  GeV [14]. Note, that the in-medium cross-section as well as the mean field can also be based on microscopic many-body approaches like Brückner theory [13,44,46–48] which is, however, not the scope of the present investigation. This approach allows to describe heavy-ion collisions at energies up to few  $A$  GeV. At higher energies the strings come into play.

The QGSM is based on the  $1/N_c$  (where  $N_c$  is the number of quark colours or flavours) topological expansion of the amplitude for processes in quantum chromodynamics and string phenomenology of particle production in inelastic binary collisions of hadrons. The diagrams of various topology, which arose due to the  $1/N_c$  expansion, correspond at high energies to processes with exchange of Regge singularities in the  $t$ -channel. For instance, planar and cylindrical diagram corresponds to the Reggeon and Pomeron exchange, respectively. Therefore, QGSM treats the elementary hadronic interactions on the basis of the Gribov-Regge theory, similar to the dual parton model [34] and the VENUS model [35]. The model simplifies the nuclear effects and concentrates on hadron rescattering. As independent degrees of freedom QGSM includes octet and nonet vector and pseudoscalar mesons, and octet and decuplet baryons, and their antiparticles.

The formation of the quark-gluon plasma is not assumed in the present version of the model. Thus, the effects similar to softening of the EOS in ultrarelativistic heavy-ion collisions, discussed below, are merely attributed to the dynamics of hadron rescattering and nuclear shadowing. We start from the study of energy and centrality dependence of the directed flow.

### III. DIRECTED FLOW

For the simulations at all three energies, namely 1A GeV, 11.6A GeV, and 160A GeV, we choose light ( $^{32}\text{S}+^{32}\text{S}$ ) and heavy ( $^{197}\text{Au}+^{197}\text{Au}$  and  $^{208}\text{Pb}+^{208}\text{Pb}$ ) symmetric systems. The directed and elliptic flow of nucleons and pions as a function of rapidity is defined as

$$v_n^i = \cos(n\phi_i) \equiv \cos(n\phi_i) \frac{d\mathcal{N}^i}{dy} dy \bigg/ \frac{d\mathcal{N}^i}{dy} dy, \quad (5)$$

where  $n = 1, 2$  and  $i = N, \pi$ . The mean directed and elliptic flow integrated over the whole rapidity range is simply

$$\langle v_n^i \rangle = \langle \cos(n\phi_i) \rangle \equiv \int \cos(n\phi_i) \frac{d\mathcal{N}^i}{dy} dy \bigg/ \int \frac{d\mathcal{N}^i}{dy} dy, \quad (6)$$

To compare different systems colliding at different energies the reduced rapidity  $\tilde{y} = y/y_{proj}$  and reduced impact parameter  $\tilde{b} = b/b_{max}$  has been used. The maximum impact parameter for a symmetric system is  $b_{max} = 2R_A$ . The value of  $\tilde{b}$  in the simulations is varying from 0.15 (central collisions) up to 0.9 (most peripheral collisions).

The rapidity distributions of  $v_1$  at SIS energies are shown in Fig. 1(a) for S+S and in Fig. 1(b) for Au+Au system. The directed flow of nucleons has a characteristic  $S$ -shape attributed to the standard  $\langle p_x/A \rangle$  distribution. Conventionally, we will call this type of flow, for which the slope  $dv_1/d\tilde{y}$  is positive, *normal* flow, in contrast to the *antiflow* for which  $dv_1/d\tilde{y} < 0$  in the midrapidity region.

The nucleon flow reaches the maximum at  $\tilde{b} = 0.3-0.45$  both in S+S and Au+Au system, and then it drops. In the midrapidity range the flow can be well approximated by a linear dependence. The slope parameters of the  $v_1^N(y)$  distributions are listed in Table I together with the  $dv_1^N/d\tilde{y}$  data at higher energies. Pions at SIS energies show only weak antiflow which reaches a maximum around  $\tilde{b} = 0.45 - 0.6$  for S+S and  $\tilde{b} = 0.6 - 0.75$  for Au+Au

collisions, i.e. in more peripheral collisions compared to the maximal nucleon directed flow. This behaviour is understandable since the evolution of a positive nuclear flow due to the (momentum dependent) repulsive  $NN$ -forces requires sufficiently large participant matter, whereas the negative pion flow due to shadowing needs large spectators. The antiflow of pions can also be fitted by a linear dependence; slope parameters are presented in Table I.

The directed flow  $v_1^i(y)$  calculated for the same systems, S+S and Au+Au, at AGS energies is shown in Fig. 2(a) and Fig. 2(b), respectively. Here the distributions for nucleons differ considerably, especially in light system, from those at 1A GeV. The deviations of  $v_1^N(y)$  from the straight line in S+S collisions begin noticeable already at  $\tilde{b} = 0.3$ . The nucleon directed flow goes to zero in the midrapidity range with increasing impact parameter. Moreover, even antiflow is developed in very peripheral collisions at  $\tilde{b} = 0.9$ , as seen in Fig. 2(a).

In contrast, in heavy Au+Au collisions at 11.6A GeV there are no singularities in the behaviour of  $v_1^N(y)$  up to  $\tilde{b} = 0.6$ . The plateau in the midrapidity region seems to build up only at  $\tilde{b} \geq 0.75$ , see Fig. 2(b). Pion directed flow has negative slope in the midrapidity range for both light and heavy colliding system. Values of the slope parameter are listed in Table I. It is worth to mention that  $v_1^\pi$  increases as the reaction becomes more peripheral, and that both pion and nucleon directed flow does not vanish even at  $\tilde{b} = 0.9$  compared to the flow at SIS energies.

At the SPS energies the directed flow of nucleons has negative slope in the midrapidity region already in semiperipheral S+S collisions as depicted in Fig. 3(a). With the increase of the impact parameter the nucleon antiflow becomes stronger. The  $y$ -dependence of  $v_1^N$  in Pb+Pb collisions is shown in Fig. 3(b). Here the deviations from the straight line start to develop at  $\tilde{b} = 0.45$  in the central rapidity window,  $|\tilde{y}| \leq 0.25$ . It is interesting that the slope of the antiflow of nucleons at  $\tilde{b} = 0.9$  is similar to that of the pion flow. The latter reaches maximum also at  $\tilde{b} = 0.9$  in Pb+Pb, as well as in S+S collisions.

The disappearance of the directed flow of hadrons can be regarded as an indication for a softening of the EOS [49,50] due to a QGP-hadron phase transition. The simple hypothesis would be that, despite the absence of the plasma formation in the microscopic model, the colour field of quark-antiquark and quark-diquark strings can force the softening of the hadronic EOS. This idea explains the disappearance of the directed flow at energies of AGS and higher, but obviously fails to explain why the effect is stronger in peripheral collisions and for light systems like S+S. The correct explanation can be, therefore, that the apparent softening of the equation of state is in fact caused by the nuclear shadowing [51,52]. The mechanism of the development of nuclear antiflow in the midrapidity range of nuclear peripheral collisions is elaborated in Sec. V.

The mean directed flow  $\langle v_1 \rangle$  of pions and nucleons is shown in Fig. 4. Except nearly central events, the pion mean flow is negative for both light and heavy colliding system at all three energies. At the AGS and SPS energies  $\langle v_1^\pi \rangle$  rises steadily as the reaction becomes more peripheral. The mean directed flow of nucleons, which is always positive, seems also to exhibit a similar tendency. The maximum in  $\langle v_1^N(\tilde{b}) \rangle$  distribution is located around  $\tilde{b} = 0.4$  for Au+Au collisions at 1A GeV. It is shifted to  $\tilde{b} = 0.6$  at 11.6A GeV, and is completely dissolved at higher energies.

#### IV. ELLIPTIC FLOW

Since the elliptic flow develops at the very beginning stage of nuclear collision, it might be even a better tool to probe the nuclear EOS under extreme conditions [53]. Particularly, calculations based on a relativistic hadron transport model indicate a transition of elliptic flow from out-of-plane to in-plane for the case of the QGP formation in Au+Au collisions in the energy range 1 – 11A GeV [54]. Recent experimental data [55] confirm the transition from negative to positive elliptic flow at  $E \approx 4A$  GeV, which was considered as indication of the softening of nuclear EOS. But can this change in the behaviour of elliptic flow be induced by some other reasons? To answer the question the microscopic study of elliptic flow of nucleons and pions has been performed at energies from 1A GeV to 160A GeV.

Figures 5(a) and 5(b) depict the elliptic flow of pions and nucleons in S+S and Au+Au collisions, respectively, at 1A GeV. The elliptic flow of pions is small and negative at  $\tilde{b} \geq 0.45$ . Nucleon elliptic flow is also negative in peripheral and semiperipheral collisions. The nucleon flow increases to maximum at  $\tilde{b} = 0.75$  and then drops. For heavy system the pionic flow is negative already at  $\tilde{b} = 0.15$ , while the nucleon flow at  $\tilde{b} \leq 0.45$  has two positive peaks, centred around  $|\tilde{y}| \approx 1.4$ , and the dip in the midrapidity region, where  $v_2^N$  is negative. In peripheral collisions the positive peaks in the  $v_2^N(y)$  distribution vanish, and the negative elliptic flow of nucleons becomes stronger. Generally, the spectator matter at target/projectile rapidities shows in-plane flow ( $v_2^N > 0$ ) whereas the participant matter at midrapidity shows preferential out-of-plane emission ( $v_2^N < 0$ ).

The elliptic flow of nucleons at the AGS energies, shown in Figs. 6(a) and 6(b), also has a two-hump structure both in S+S and in Au+Au collisions. But in Au+Au interactions the nucleon flow becomes negative in the central part of  $\tilde{y}$ -distribution only at  $\tilde{b} \geq 0.75$ . The peaks are quite noticeable and shifted closer to the center of the distributions. In Au+Au collisions the elliptic flow of both pions and nucleons is at least twice as large as in S+S interactions. At  $\tilde{b} \leq 0.6$  the nucleon flow is positive, while the pionic flow becomes negative at midrapidity already at  $\tilde{b} = 0.45$ .

At the SPS energies the elliptic flow of pions in S+S collisions is quite flat and slightly positive, as demonstrated in Fig. 7(a). The flow of nucleons in this reaction is also small and positive except for  $\tilde{b} \geq 0.75$ , where the negative dip around  $\tilde{y} = 0$  is built up. The negative flow is seen for nucleons in Pb+Pb interactions only at  $\tilde{b} = 0.9$  in Fig. 7(b). The origin of the negative values of  $v_2^N$  at midrapidity can be linked to absorption of hadrons, emitted at  $\theta = 90^\circ$  angle in the reaction plane, by the dense baryon rich spectators, while hadrons emitted out-of-plane remain almost unaffected. Note also that the positions of positive maxima in  $v_2^N(y)$  distributions in Pb+Pb reactions are shifted to  $\tilde{y} \approx 0.45$ . Compared to  $v_2^\pi$  in S+S interactions, the elliptic flow of pions in Pb+Pb collisions is large and positive. It has a noticeable dip at midrapidity only in very peripheral collisions.

The  $\tilde{b}$ -dependence of elliptic flow integrated over the whole rapidity range is presented in Fig. 8. In S+S collisions the mean elliptic flow of pions is quite weak for all three energies, though it appears to change the sign from negative at 1A GeV to positive at 160A GeV. The nucleon flow in S+S reaction is more distinct. It is negative at the SIS energies, while at both AGS and SPS energies  $\langle v_2^N(\tilde{b}) \rangle$  is positive and almost constant.

The situation is changed drastically with the rise of the mass number of colliding nuclei from  $A = 32$  to  $A = 197(208)$ . The mean elliptic flow of pions becomes positive at the AGS

energies, in accord with the experimental results [55]. The flow reaches maximum values at  $160A$  GeV. It is easy to see that the strength of  $\langle v_2^\pi(b) \rangle$  increases with  $\tilde{b}$  rising to 0.75, which corresponds to  $b = 10$  fm in the calculations, and then drops. At the SIS energies the nucleon mean elliptic flow is positive in semicentral and semiperipheral events with  $\tilde{b} \leq 0.45$  and negative at higher values of the impact parameter. Thus in the heavy system there appears a transition of in-plane to out-of-plane flow with decreasing centrality of the reaction. A detailed analysis of the EOS dependence on the nuclear mean field at SIS energies will be presented elsewhere. The nucleon flow has the maximum strength at  $11.6A$  GeV, in contrast to the pion mean elliptic flow which rises continuously with increasing incident energy.

## V. DISCUSSION OF THE RESULTS

We see in Sec. III that directed flow of nucleons in (semi)peripheral heavy-ion collisions noticeably deviates from the straight line behaviour in the midrapidity range at AGS energies or higher. The comparison between light and heavy systems colliding at the same energy per nucleon shows that the effect is stronger in the light system. The most probable explanation of this phenomenon is nuclear shadowing. To clarify the idea the symmetric system of two nuclei at maximum overlap is shown in Fig. 9 for the three energies under consideration. In addition, Fig. 10 illustrates the development of the antiflow-like behaviour in the midrapidity region. As was discussed in, e.g. [51,52], the total flow of hadrons is a result of mutual cancellation of two competitive components, namely, the normal flow which follows the ongoing spectators, and the antiflow which develops towards the baryon dilute areas of collision. The normal flow integrated over the whole rapidity range is always slightly larger than the integrated antiflow. But in the midrapidity window the antiflow can dominate over its normal counterpart. For instance, hadrons with small rapidities, emitted early in the direction of normal flow in heavy-ion collision at  $160A$  GeV, (see Fig. 10) will be absorbed by flying spectators. In contrast, hadrons, emitted in the direction of antiflow even at the angles close to  $\theta = 90^\circ$  to the beam axis, propagate freely.

This effect can be reduced by (i) increasing the centrality of the collision and (ii) by decreasing the center-of-mass energy of colliding nuclei (see Fig. 9). In both cases the area where particles can be emitted without shadowing significantly shrinks. It is important to mention here that in heavy-ion collisions at collider energies, RHIC ( $\sqrt{s} = 200$  GeV) and LHC ( $\sqrt{s} = 5.5$  TeV), the disappearance of nucleon directed flow in the midrapidity range should emerge already in semicentral collisions with  $b \leq 3$  fm.

But why the irregularities in  $v_1^N(y)$ -distribution start to develop in light system at smaller impact parameter compared to that of heavy system? To answer this question note that the larger volume of overlapping zone in heavy system leads to the intensive rescattering of baryons and increase of hadron emission from the central fireball. The spectators still absorb several early emitted hadrons, but this process becomes less efficient compared to that of the light system, where the isotropic particle radiation from the central part is not so strong. Since the effect can be misinterpreted as an evidence for the QGP formation, it should be subtracted from the analysis of experimental data.

The presence of spectators, which absorb hadrons early emitted in the direction of normal flow, affects also the development of elliptic flow. Particularly, it leads to the creation of the



dip in  $v_2(y)$  in midrapidity range. As expected from simple geometrical considerations, the effect is stronger in peripheral collisions.

The transition of elliptic flow from the out-of-plane to in-plane direction with the rise of energy from  $1A$  GeV to  $11.6A$  GeV can also be linked to change in geometry of colliding system. The Lorentz-contracted spectators, which rapidly fly away, provide more free space for the in-plane development of the flow than almost noncontracted nuclei, see Figs. 9 and 10.

It is worth to mention that the elliptic flow of nucleons as a function of impact parameter becomes more flat with rising energy of the collision, while the maximum in  $v_2^\pi(b)$  distribution is shifted to very peripheral events. This tendency is clearly seen in Fig. 8. Figure 11 presents the comparison of the model simulations of the elliptic flow of charged pions in  $3 < y < 6$  in Pb+Pb collisions at SPS energies with the experimental data [56]. We see that the QGSM provides a good quantitative agreement with the experiment. Note that the behaviour of the elliptic flow of charged particles is determined by the proton elliptic flow at energies below  $11.6A$  GeV and by the pionic elliptic flow at  $160A$  GeV. It means that although the physics of rescattering in the QGSM is the same in peripheral and central collisions, the nuclear matter undergoes a transition from a baryon dominated to a meson dominated matter with rising energy of colliding nuclei. The transition is similar to the predicted in [57] transition from hadronic to partonic degrees of freedom.

## VI. CONCLUSIONS

The directed and elliptic flow of hadrons in heavy-ion collisions is very sensitive to the EOS of the nuclear medium. At low and intermediate energies (SIS) hadrons are the relevant degrees of freedom, and the intranuclear interactions, i.e. the mean field, determine the EOS as well as the reaction dynamics. With increasing energy new degrees of freedom are extended, and the formation of small domains of a QGP phase might happen already at the SPS energies or even below. Accompanied by the phase transition to the hadronic phase this enforces a softening of the EOS due to the dropping pressure. Thus, the disappearance of the directed flow in midrapidity range can be considered as an indication of a new state of matter. This conclusion is supported by hydrodynamic simulations. No deviations of the nucleon directed flow from the straight line in  $|\tilde{y}| \leq 1$  range have been found in the one-fluid calculations with a pure hadronic EOS [58,59].

On the other hand, several microscopic models, which do not explicitly imply the QGP formation, predict larger or smaller deviations of the directed flow from the straight line behaviour [51,52,60,61] which is presented at low and intermediate energies. These deviations are attributed to the shadowing effect, which plays a decisive role in the competition between normal flow and antiflow in (semi)peripheral ultrarelativistic collisions of nuclei. Hadrons, emitted with small rapidities at the onset of the collision in the antiflow area can propagate freely, while their counterparts will be absorbed by the flying massive spectators.

The signal becomes stronger with the rise of the impact parameter. In collisions with the same impact parameter the antiflow starts to dominate over the normal flow in the midrapidity range as the reaction becomes more energetic, i.e. the spectators are more Lorentz-contracted and more hadrons can be emitted unscreened with small rapidities in the direction of antiflow. Therefore, this effect should appear in (semi)central collisions with

$b \leq 3$  fm at RHIC energies, and can imitate the softening of the EOS of hot and dense nuclear matter. However, the disappearance of directed flow due to shadowing is more distinct for light systems, like S+S or Ca+Ca, colliding with the same reduced impact parameter. In the case of a plasma creation the effect should be more pronounced in large systems like Pb+Pb. Thus, one can distinguish between the two phenomena, shadowing and quark-hadron phase transition, by the comparison of the directed flow of nucleons in the midrapidity range in light and heavy-ion collisions.

The elliptic flow of nucleons and pions is found to change its orientation from out-of-plane at  $1A$  GeV to in-plane at  $11.6A$  GeV. Since the dynamics of rescattering is the same, the effect can be explained by purely geometric reasons, such as stronger Lorentz-contraction of colliding nuclei. At higher colliding energies the contracted spectators leave the reaction zone faster, thus giving space for the growth of elliptic flow in the reaction plane.

Results of the simulations appear to favour a similarity of hadron rescattering in central and peripheral heavy-ion collisions at energies up to  $160A$  GeV. QGSM predicts that the  $\langle v_2^\pi(b) \rangle$ -distribution in Pb+Pb collisions at SPS energies increases as the reaction becomes more peripheral, in accord with the experimental data. The elliptic flow of pions in this reaction drops only for highly peripheral collisions somewhere at  $b \approx 12$  fm. However, if the data will show the further rise of elliptic flow even at such impact parameters, this can be taken as an indication for new processes not included in present version of the model. The situation awaits better data on both directed and elliptic flow in the midrapidity range and in very peripheral collisions of light and heavy nuclei at ultrarelativistic energies.

**Acknowledgements.** We are thankful to L. Csernai, E. Shuryak, H. Sorge, H. Stöcker, S. Voloshin, and Nu Xu for the fruitful discussions and comments. This work was supported in part by the Bundesministerium für Bildung und Forschung (BMBF) under contract 06TÜ887.

## REFERENCES

- [1] Proceedings of the QM'97 conference, Nucl. Phys. **A638** (1998).
- [2] Proceedings of the QM'99 conference, Nucl. Phys. **A** (in press).
- [3] H. Stöcker and W. Greiner, Phys. Rep. **137**, 277 (1986).
- [4] W. Reisdorf and H.G. Ritter, Annu. Rev. Nucl. Part. Sci. **47**, 663 (1997).
- [5] J.-Y. Ollitrault, Nucl. Phys. **A638**, 195c (1998).
- [6] W. Sheid, H. Müller, and W. Greiner, Phys. Rev. Lett. **32**, 741 (1974).
- [7] P. Danielewicz and G. Odyniec, Phys. Lett. B **157**, 146 (1985).
- [8] H.-Å. Gustafsson *et al.*, Phys. Rev. Lett. **52** (1984) 1590.
- [9] R.E. Renfordt *et al.*, Phys. Rev. Lett. **53** (1984) 763.
- [10] H. Appelshäuser *et al.*, NA49 Collab., Phys. Rev. Lett. **80** (1998) 4136.
- [11] M.M. Aggarwal *et al.*, WA98 Collab., Phys. Rev. Lett. (submitted) (nucl-ex/9807004v2).
- [12] J. Aichelin, Phys. Rep. **202**, 233 (1991).
- [13] C. Fuchs, E. Lehmann, R. Puri, L. Sehn, Amand Faessler, H.H. Wolter, J. Phys. G **22**, 131 (1996).
- [14] N. Bastid *et al.*, FOPI Collab., Nucl. Phys. **A622**, 573 (1997);  
P. Crochet *et al.*, FOPI Collab., Nucl. Phys. **A624**, 755 (1997); *ibid* **A627**, 522 (1997).
- [15] N.S. Amelin, E.F. Staubo, L.P. Csernai, V.D. Toneev, K.K. Gudima, and D. Strottman, Phys. Rev. Lett. **67**, 1523 (1991).
- [16] L.V. Bravina, L.P. Csernai, P. Lévai, and D. Strottman, Phys. Rev. C **50**, 2161 (1994);  
L.V. Bravina, N.S. Amelin, L.P. Csernai, P. Lévai, and D. Strottman, Nucl. Phys. **A566**, 461c (1994).
- [17] J. Brachmann, S. Soff, A. Dumitru, H. Stöcker, J.A. Maruhn, L.V. Bravina, W. Greiner, and D.H. Rischke, Phys. Rev. C **61**, 024909 (2000).
- [18] S. Voloshin and Y. Zhang, Z. Phys. C **70**, 665 (1996).
- [19] S.A. Voloshin, Phys. Rev. C **55**, R1630 (1997).
- [20] A.M. Poskanzer and S.A. Voloshin, Phys. Rev. C **58**, 1671 (1998).
- [21] J.-Y. Ollitrault, Phys. Rev. D **46**, 229 (1992).
- [22] J. Barrette *et al.*, E877 Collab., Phys. Rev. Lett. **73** (1994) 2532.
- [23] S. Nishimura *et al.*, WA98 Collab., Nucl. Phys. A **638**, 459c (1998).
- [24] H. Sorge, Phys. Lett. B **402**, 251 (1997).
- [25] P.F. Kolb, J. Sollfrank, and U. Heinz, Phys. Lett. B **459**, 667 (1999).
- [26] H. Sorge, Phys. Rev. Lett. **82**, 2048 (1999).
- [27] H. Heisenberg and A.-M. Levy, Phys. Rev. C **59**, 2716 (1999).
- [28] L.D. Landau and E.M. Lifshiz, *Fluid Dynamics* (Pergamon Press, New York, 1959).
- [29] H. von Gersdorff, M. Kataja, L. McLerran, and P.V. Ruuskanen, Phys. Rev. D **34**, 794 (1986).
- [30] R.B. Clare and D. Strottman, Phys. Rep. **141**, 179 (1986).
- [31] I.N. Mishustin, V.N. Russkikh, and L.M. Satarov, Nucl. Phys. **A494**, 595 (1989).
- [32] J. Brachmann, A. Dumitru, J.A. Maruhn, H. Stöcker, W. Greiner, and D.H. Rischke, Nucl. Phys. **A619**, 391 (1997).
- [33] B. Andersson, G. Gustafson, and B. Nilsson-Almqvist, Nucl. Phys. B **281**, 289 (1987);  
T. Sjöstrand, preprint CERN-TH 7112/93 (1993).
- [34] A. Capella, U. Sukhatme, C.I. Tan, and J.T.T. Van, Phys. Rep. **236**, 225 (1994).
- [35] K. Werner, Phys. Rep. **232**, 87 (1993).

- [36] N.S. Amelin, L.V. Bravina, L.I. Sarycheva, and L.N. Smirnova, *Sov. J. Nucl. Phys.* **50**, 1058 (1989);  
N.S. Amelin and L.V. Bravina, *Sov. J. Nucl. Phys.* **51**, 133 (1990);  
N.S. Amelin, L.V. Bravina, L.P. Csernai, V.D. Toneev, K.K. Gudima, and S.Yu. Sivoklov, *Phys. Rev. C* **47**, 2299 (1993).
- [37] H. Sorge, H. Stöcker, and W. Greiner, *Ann. Phys.* **192**, 266 (1989).
- [38] M.Gyulassy and X.-N. Wang, *Comp. Phys. Commun.* **83**, 307 (1994).
- [39] K. Geiger, *Phys. Rep.* **258**, 237 (1995).
- [40] B.A. Li and C.M. Ko, *Phys. Rev. C* **52**, 2037 (1995).
- [41] S.A. Bass, M. Belkacem, M. Bleicher, M. Brandstetter, L. Bravina, C. Ernst, L. Gerland, M. Hofmann, S. Hofmann, J. Konopka, G. Mao, L. Neise, S. Soff, C. Spieles, H. Weber, L.A. Winkelmann, H. Stöcker, W. Greiner, Ch. Hartnack, J. Aichelin, and N. Amelin, *Prog. Part. Nucl. Phys.* **41**, 255 (1998);  
M. Bleicher, E. Zabrodin, C. Spieles, S.A. Bass, C. Ernst, S. Soff, L. Bravina, M. Belkacem, H. Weber, H. Stöcker, and W. Greiner, *J. Phys. G* **25**, 1859 (1999).
- [42] S.A. Bass, M. Hofmann, M. Bleicher, L. Bravina, E. Zabrodin, H. Stöcker, and W. Greiner, *Phys. Rev. C* **60**, 021901 (1999).
- [43] S.A. Bass, A. Dumitru, M. Bleicher, L. Bravina, E. Zabrodin, H. Stöcker, and W. Greiner, *Phys. Rev. C* **60**, 021902 (1999).
- [44] G. Batko, Amand Faessler, S.W. Huang, E. Lehmann, and R.K. Puri, *J. Phys. G* **20**, 461 (1994).
- [45] V.S. Uma Maheswari, C. Fuchs, Amand Faessler, L. Sehn, D. Kosov, Z. Wang, *Nucl. Phys.* **A628**, 669 (1998).
- [46] J. Jaenicke, J. Aichelin, N. Ohtsuka, R. Linden, and Amand Faessler, *Nucl. Phys.* **A536**, 201 (1992).
- [47] T. Gross-Boelting, C. Fuchs, and Amand Faessler, *Nucl. Phys.* **A648**, 105 (1999).
- [48] T. Gaitanos, C. Fuchs, H. H. Wolter, *Nucl. Phys.* **A650**, 97 (1999).
- [49] C.M. Hung and E.V. Shuryak, *Phys. Rev. Lett* **75**, 4003 (1995).
- [50] D.H. Rischke and M. Gyulassy, *Nucl. Phys.* **A597**, 701 (1996).
- [51] L.V. Bravina, *Phys. Lett. B* **344**, 49 (1995).
- [52] L.V. Bravina, E.E. Zabrodin, Amand Faessler, and C. Fuchs, *Phys. Lett. B* **470**, 27 (1999) (nucl-th/9911012).
- [53] P. Danielewicz, *Nucl. Phys.* **A** (in press) (nucl-th/9907098).
- [54] P. Danielewicz, R.A. Lacey, P.-B. Gossiaux, C. Pinkenburg, P. Chung, J.M. Alexander, and R.L. McGrath, *Phys. Rev. Lett.* **81**, 2438 (1998).
- [55] C. Pinkenburg *et al.*, E895 Collab., *Phys. Rev. Lett.* **83**, 1295 (1999).
- [56] A.M. Poskanzer and S.A. Voloshin for the NA49 Collab., *Nucl. Phys. A* (in press) (nucl-ex/9906013).
- [57] A.M. Poskanzer and S.A. Voloshin, nucl-th/9906075.
- [58] L.P. Csernai, *Introduction to Relativistic Heavy Ion Collisions* (Wiley, New York, 1994).
- [59] L.P. Csernai and D. Röhrich, *Phys. Lett. B* **458**, 454 (1999).
- [60] H. Liu, S. Panitkin, and N. Xu, *Phys. Rev. C* **59**, 348 (1999).
- [61] R.J.M. Snellings, H. Sorge, S.A. Voloshin, F.Q. Wang, and N. Xu, *Phys. Rev. Lett.* (in press) (nucl-ex/9908001).

FIGURES

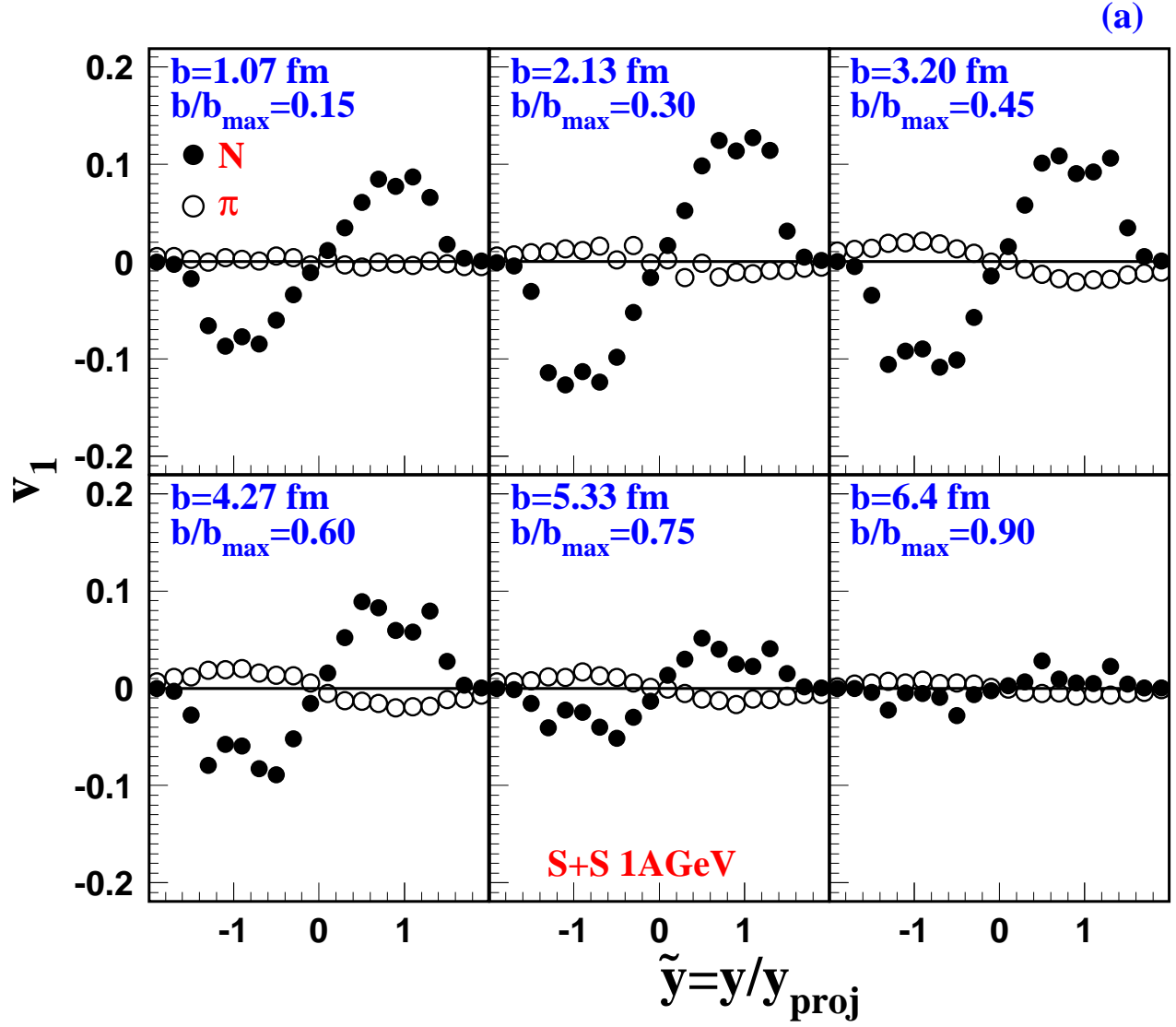
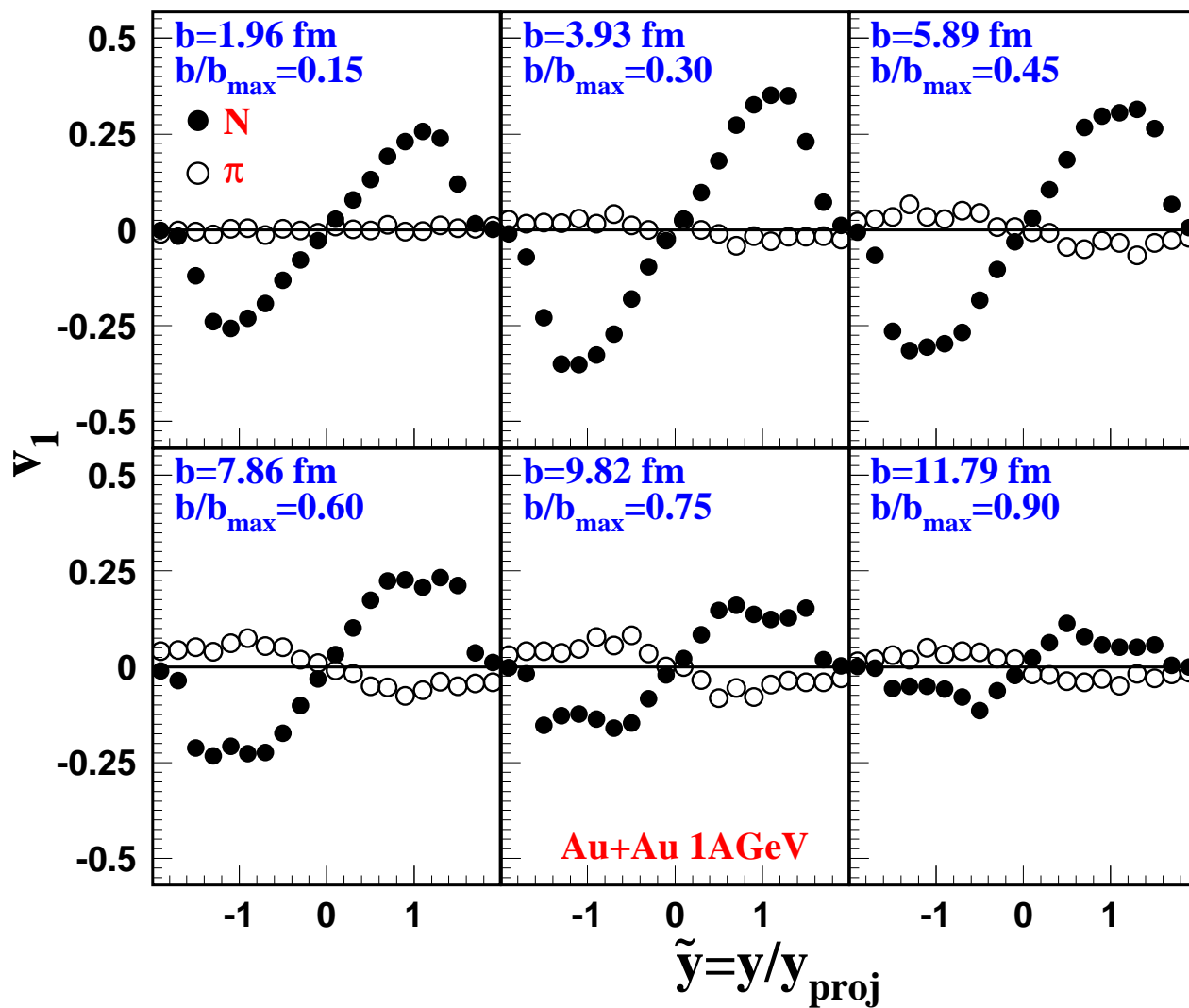


FIG. 1. (a) Directed flow of nucleons (full circles) and pions (open circles) as a function of rapidity in  $^{32}\text{S}+^{32}\text{S}$  collisions at 1A GeV.  
 (b) the same as (a) but for  $^{197}\text{Au}+^{197}\text{Au}$  collisions.

(b)



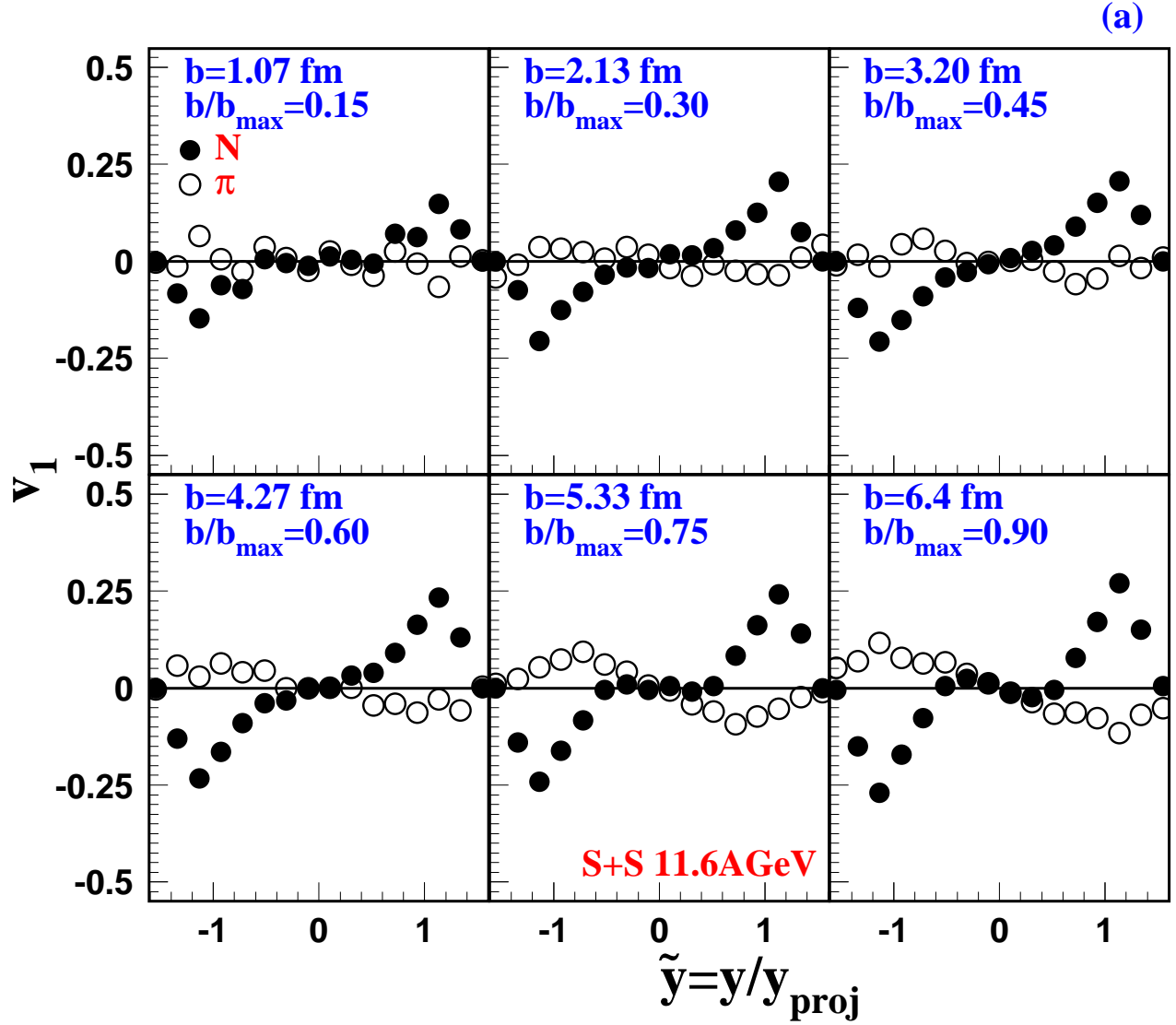
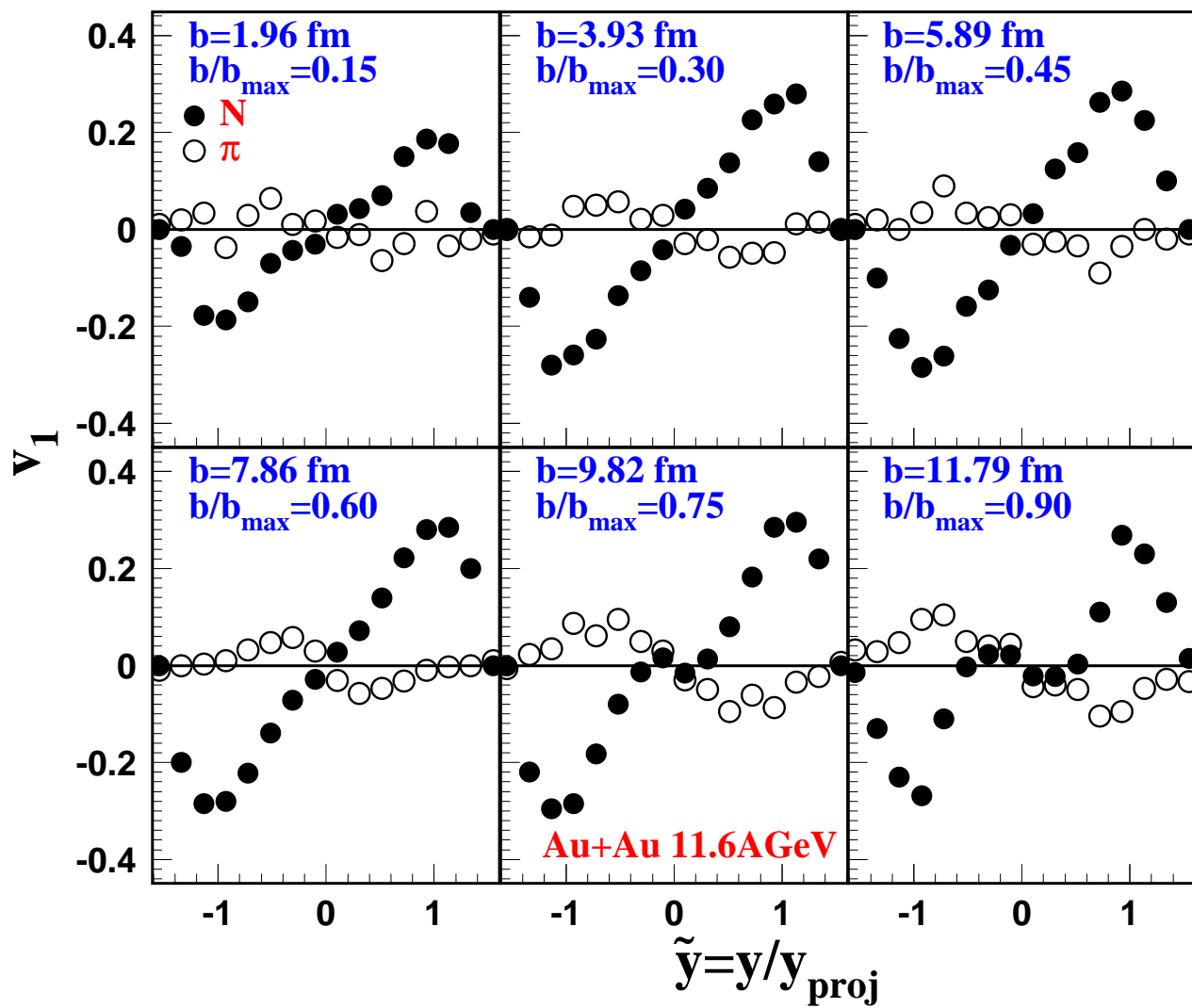


FIG. 2. (a) Directed flow of nucleons (full circles) and pions (open circles) as a function of rapidity in  $^{32}\text{S}+^{32}\text{S}$  collisions at 11.6A GeV.  
 (b) the same as (a) but for  $^{197}\text{Au}+^{197}\text{Au}$  collisions.

(b)





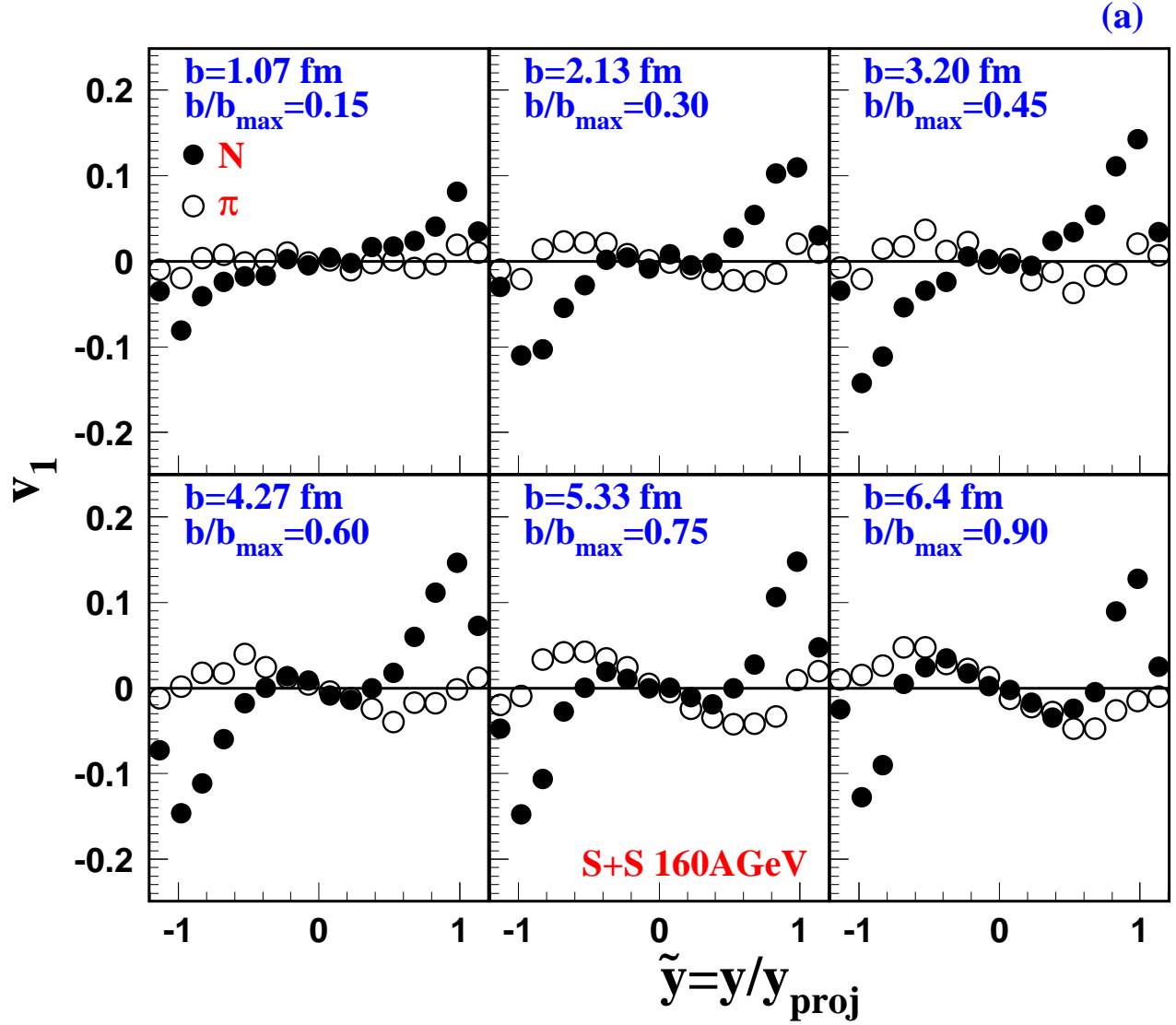
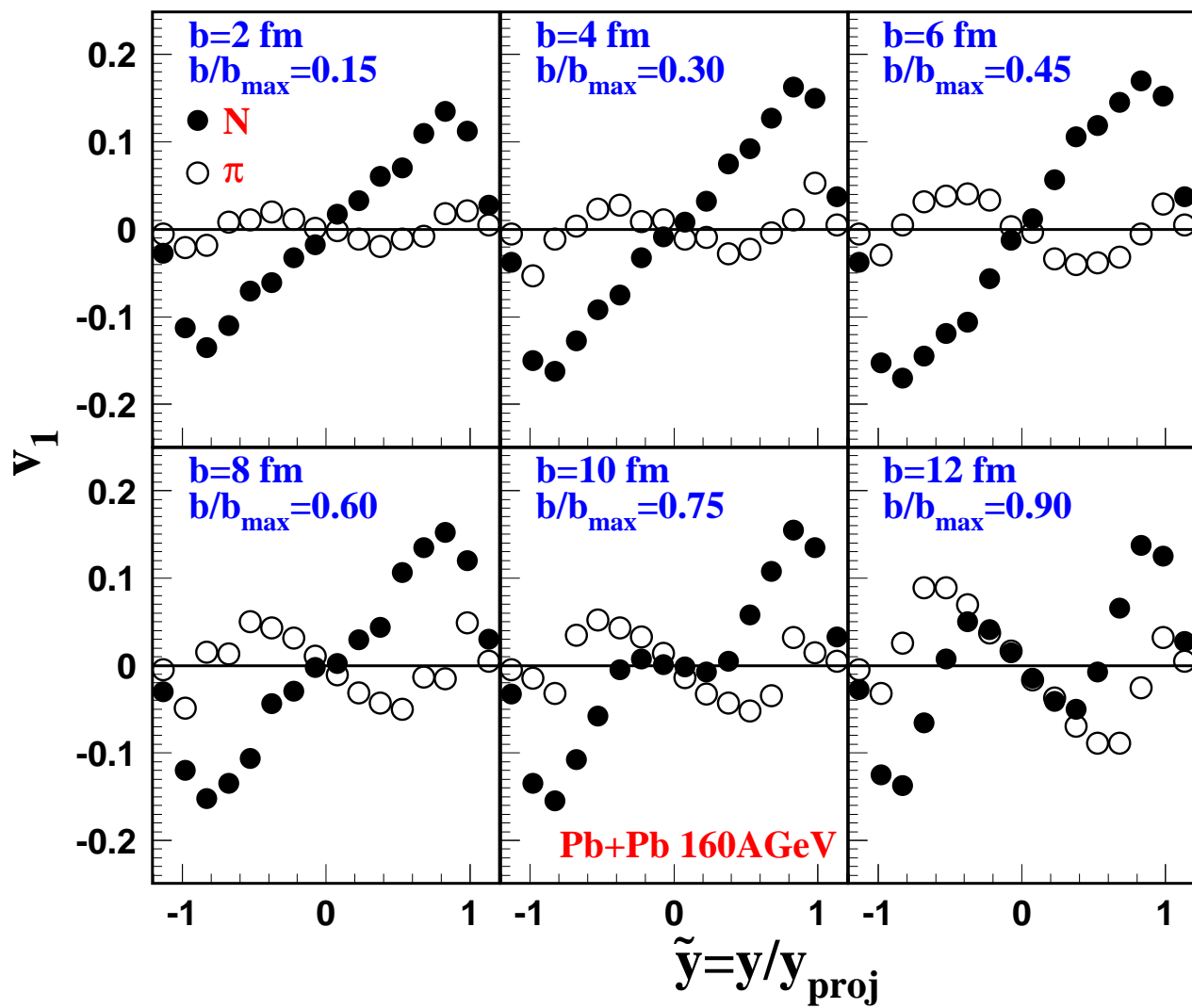


FIG. 3. (a) Directed flow of nucleons (full circles) and pions (open circles) as a function of rapidity in  $^{32}\text{S}+^{32}\text{S}$  collisions at  $160A$  GeV. (b) the same as (a) but for  $^{208}\text{Pb}+^{208}\text{Pb}$  collisions.

(b)



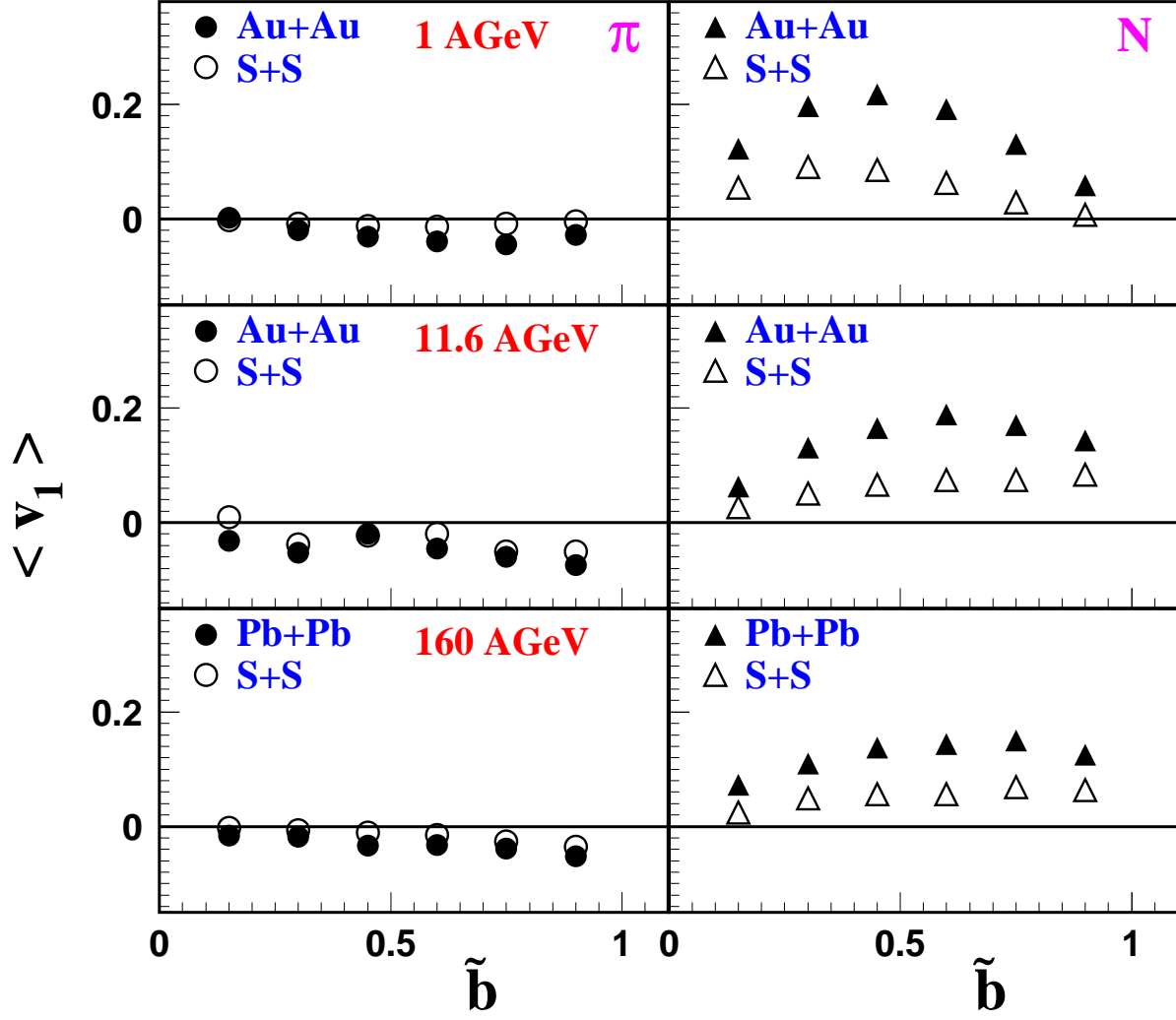


FIG. 4. The mean directed flow of nucleons (full circles) and pions (open circles) in light and heavy system colliding at  $1A$  GeV,  $11.6A$  GeV, and  $160A$  GeV, respectively.

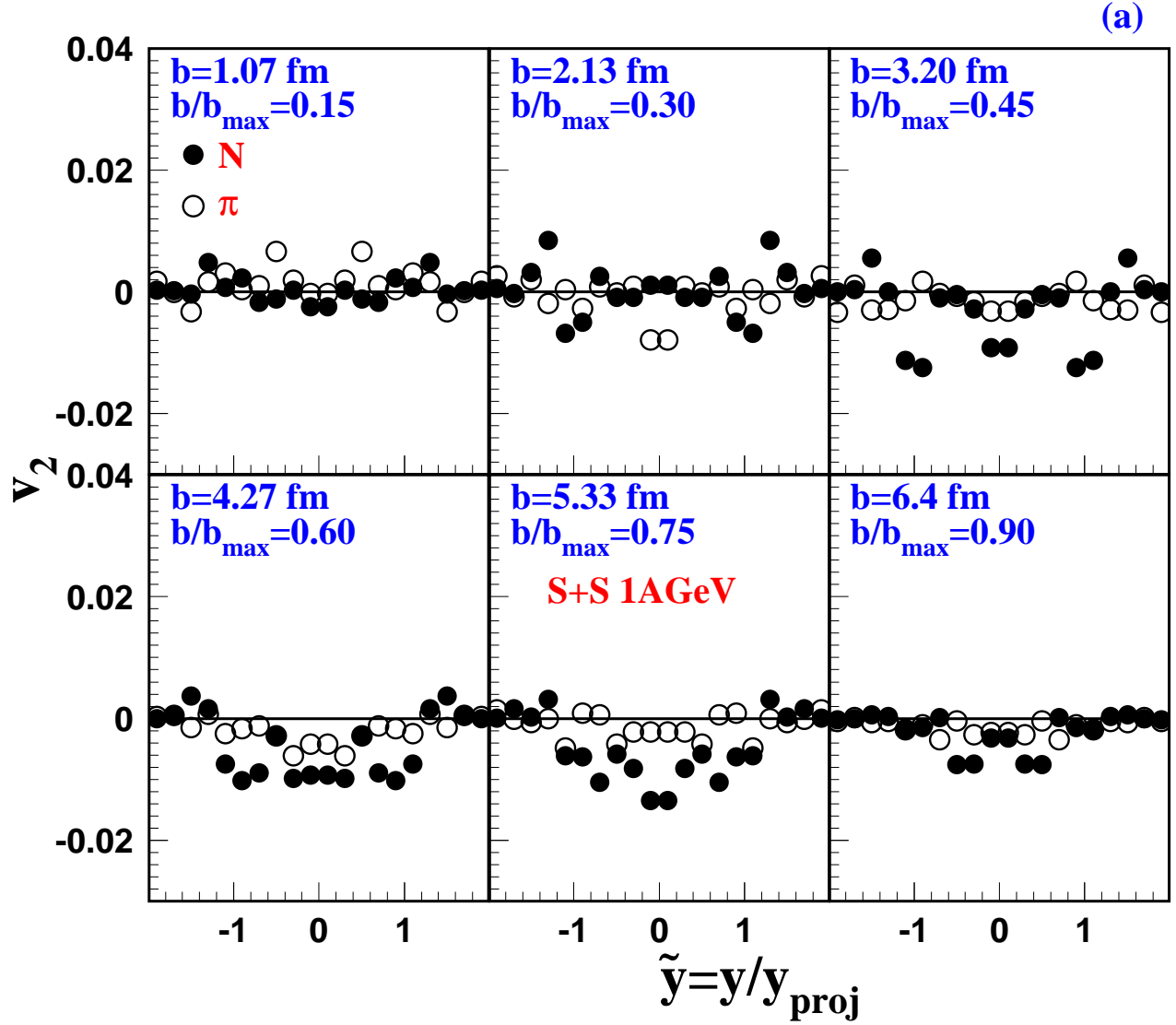
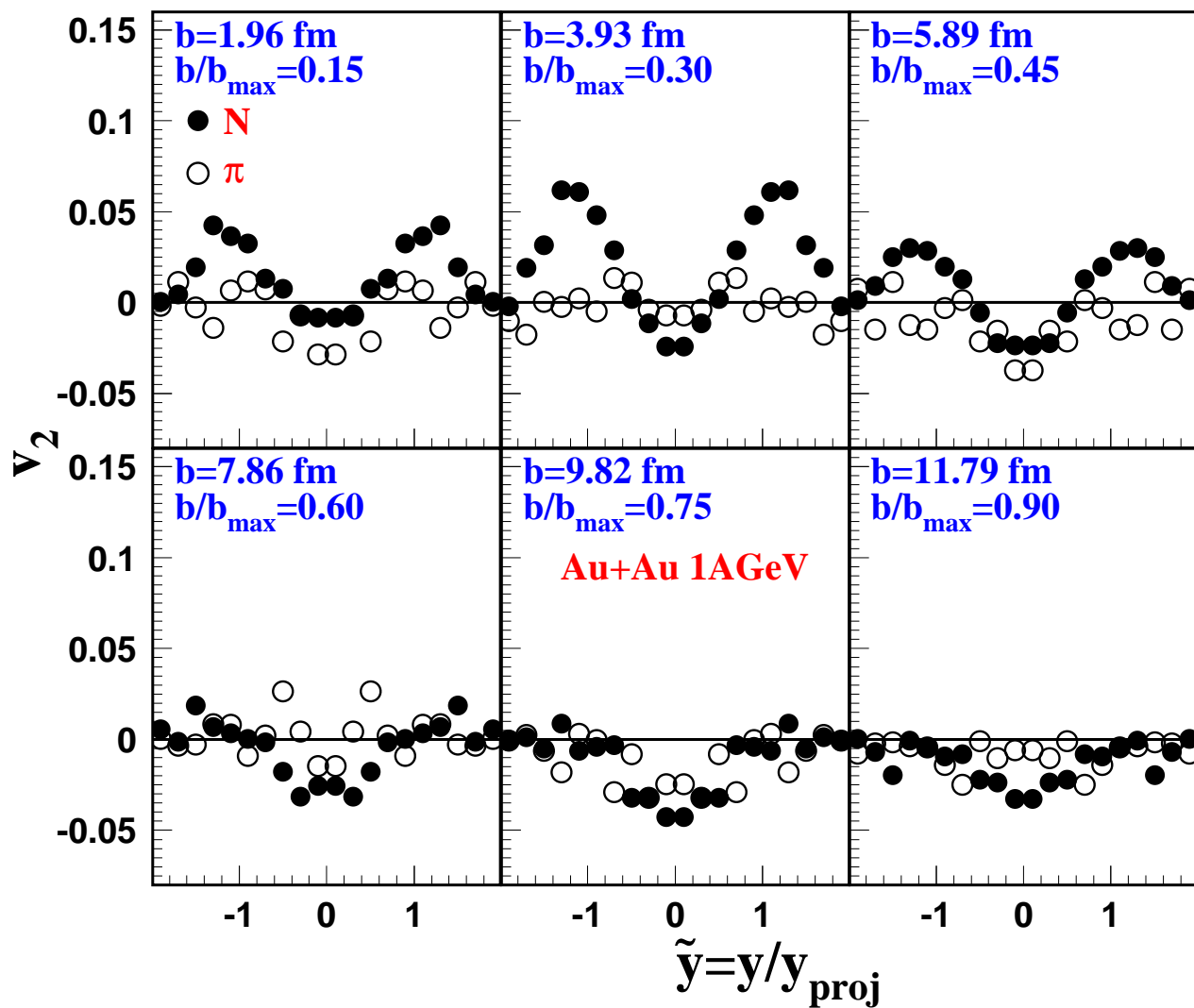


FIG. 5. (a) Elliptic flow of nucleons (full circles) and pions (open circles) as a function of rapidity in  $^{32}\text{S}+^{32}\text{S}$  collisions at 1A GeV.  
 (b) the same as (a) but for  $^{197}\text{Au}+^{197}\text{Au}$  collisions.

(b)



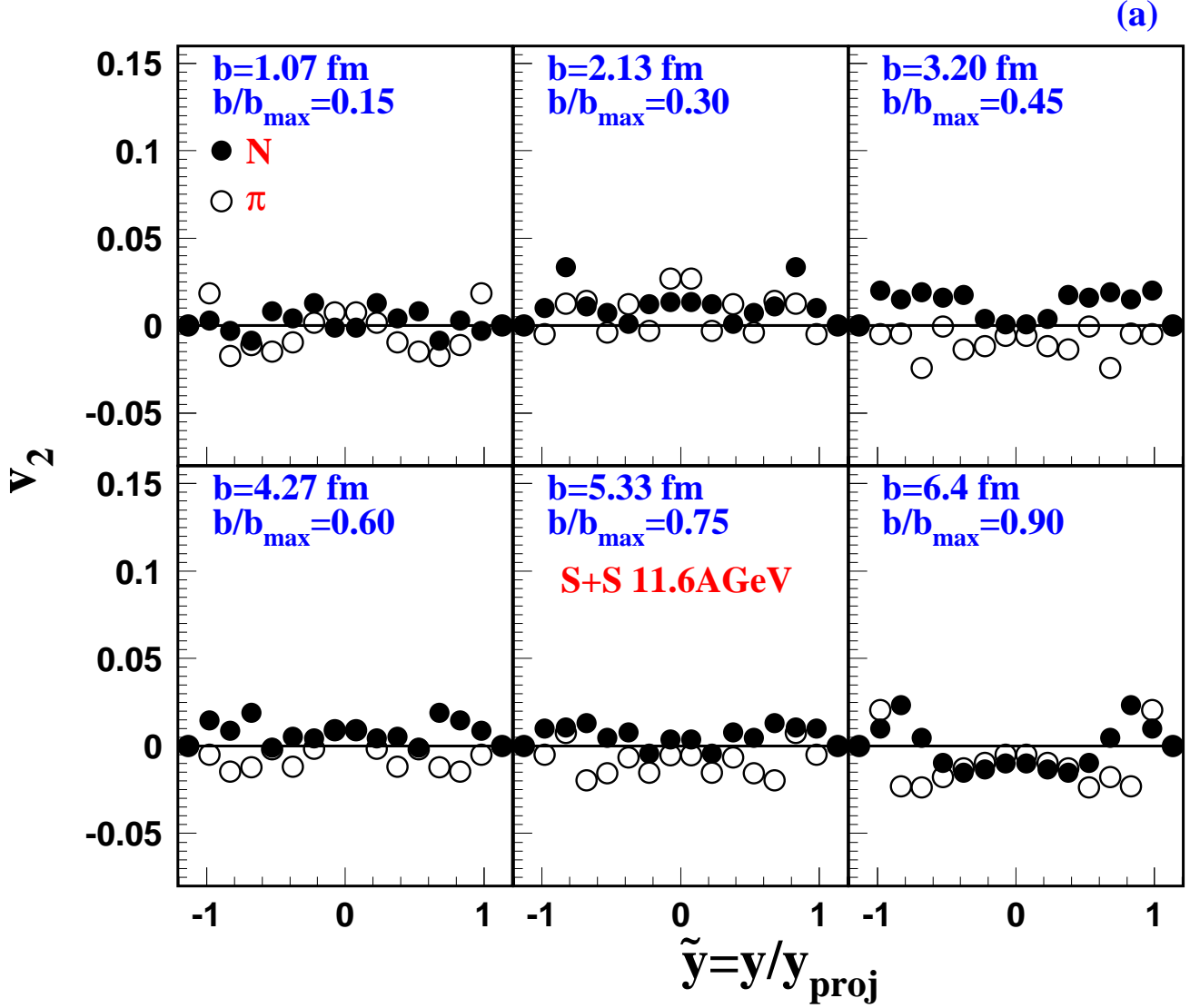
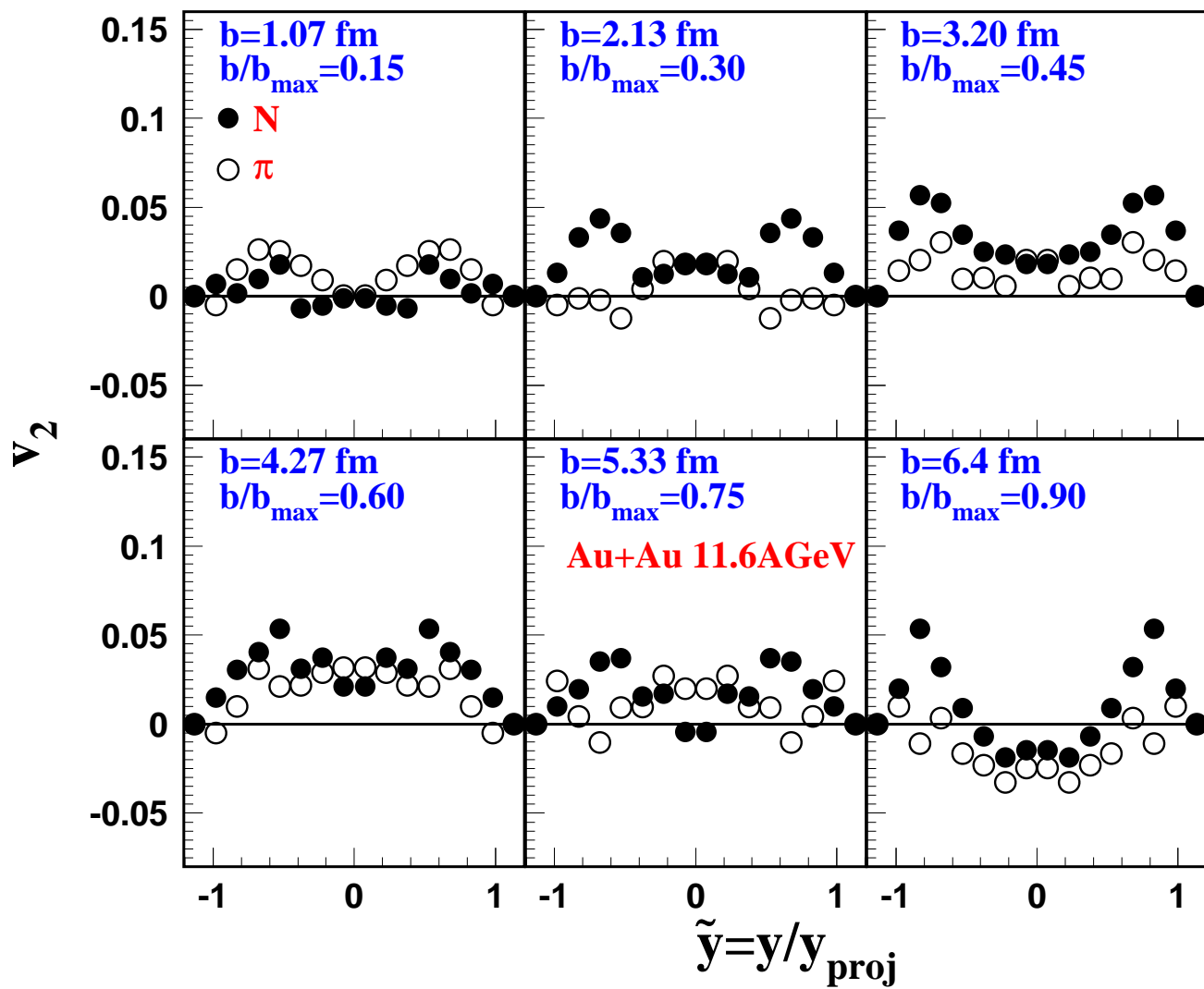


FIG. 6. (a) Elliptic flow of nucleons (full circles) and pions (open circles) as a function of rapidity in  $^{32}\text{S}+^{32}\text{S}$  collisions at  $11.6A$  GeV.  
 (b) the same as (a) but for  $^{197}\text{Au}+^{197}\text{Au}$  collisions.

(b)



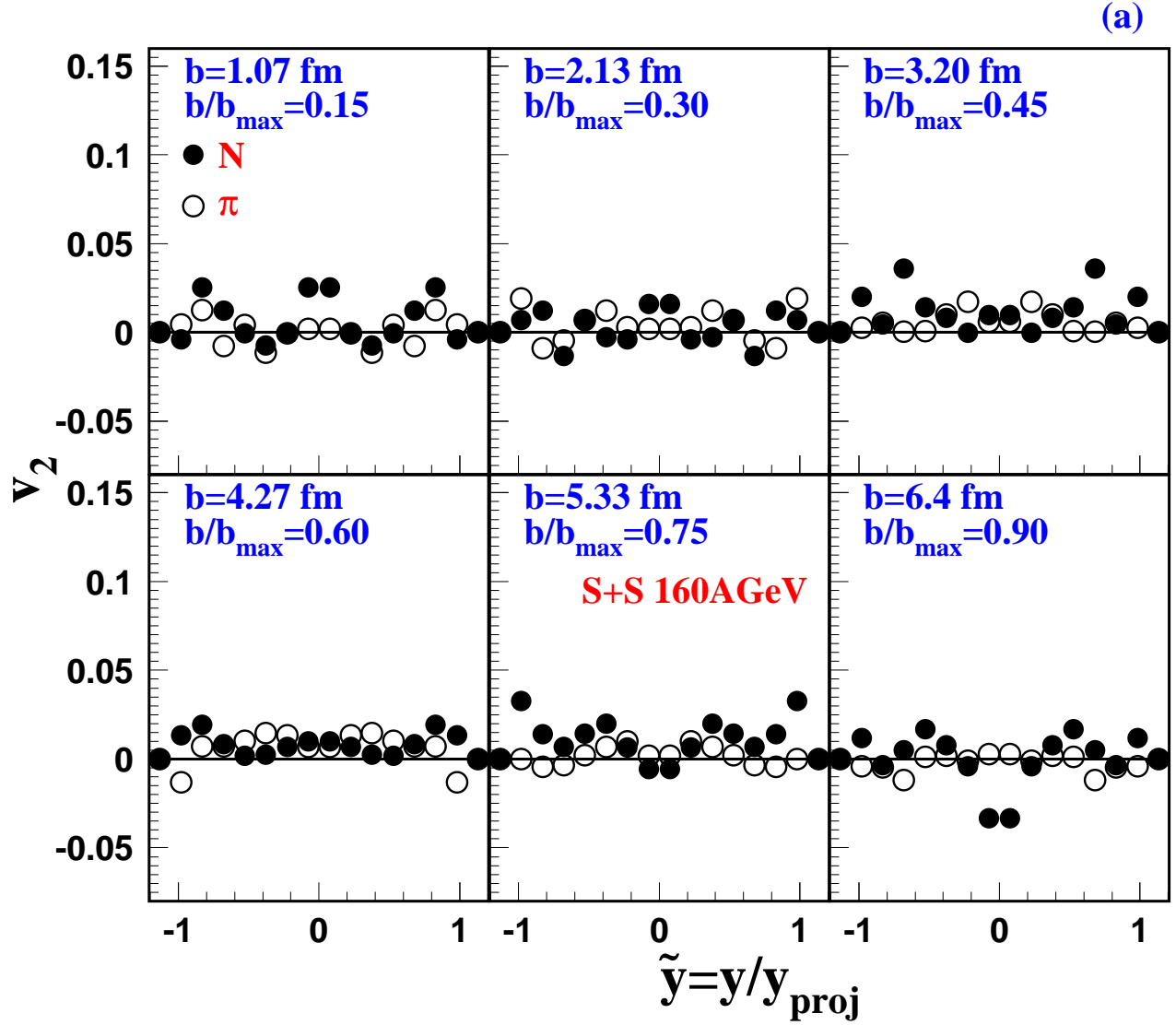
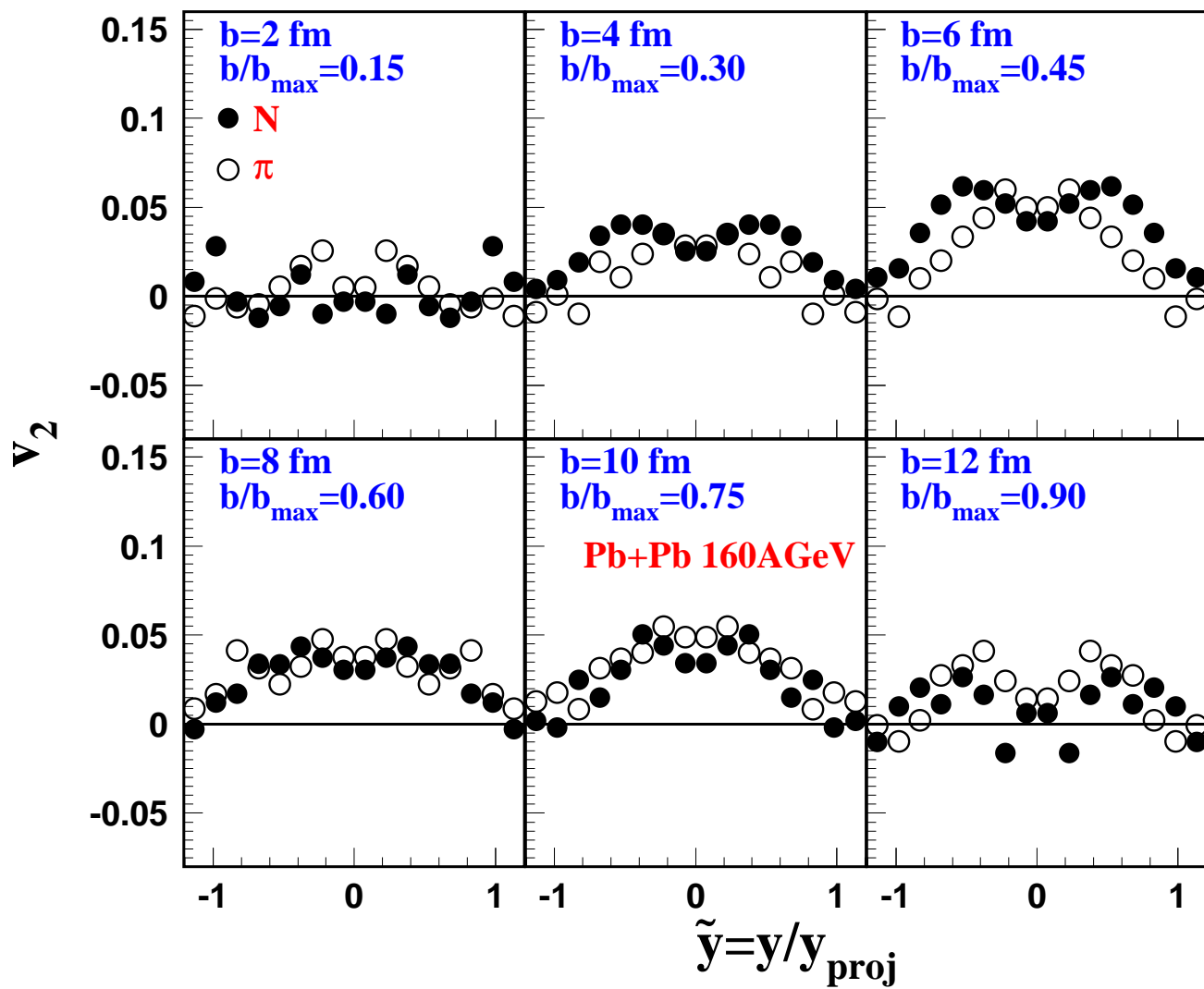


FIG. 7. (a) Elliptic flow of nucleons (full circles) and pions (open circles) as a function of rapidity in  $^{32}\text{S}+^{32}\text{S}$  collisions at  $160A$  GeV.  
 (b) the same as (a) but for  $^{208}\text{Pb}+^{208}\text{Pb}$  collisions.



(b)



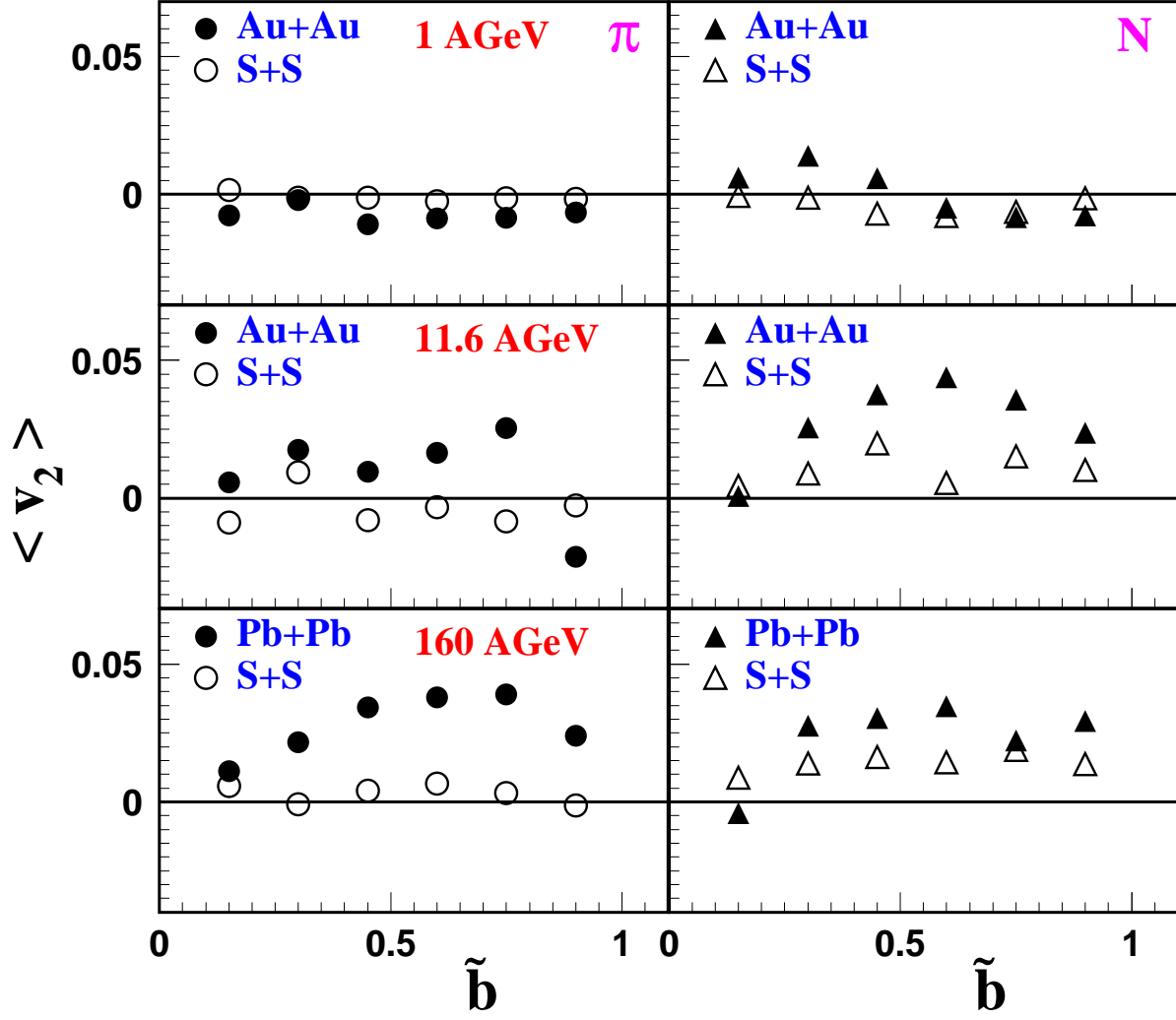


FIG. 8. The mean directed flow of nucleons (triangles) and pions (circles) in light (open symbols) and heavy (full symbols) system colliding at 1A GeV, 11.6A GeV, and 160A GeV, respectively.

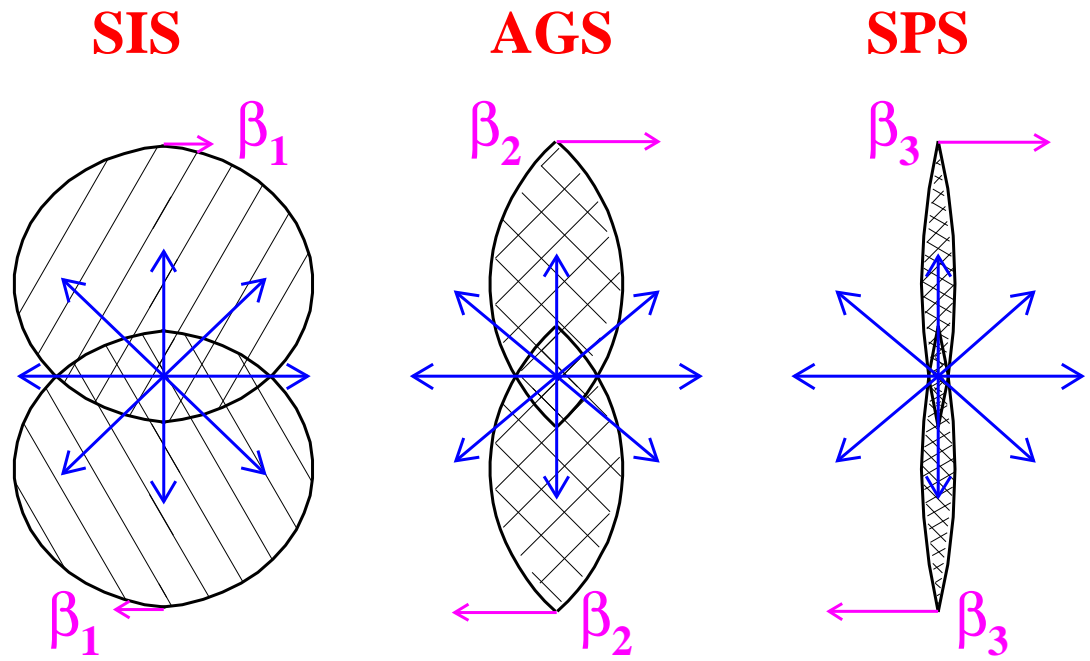


FIG. 9. Symmetric system of colliding nuclei at maximum overlap shown in  $(x,z)$ -plane at SIS, AGS, and SPS energies, respectively. Arrows indicate the possible directions of particle emission from the central zone.

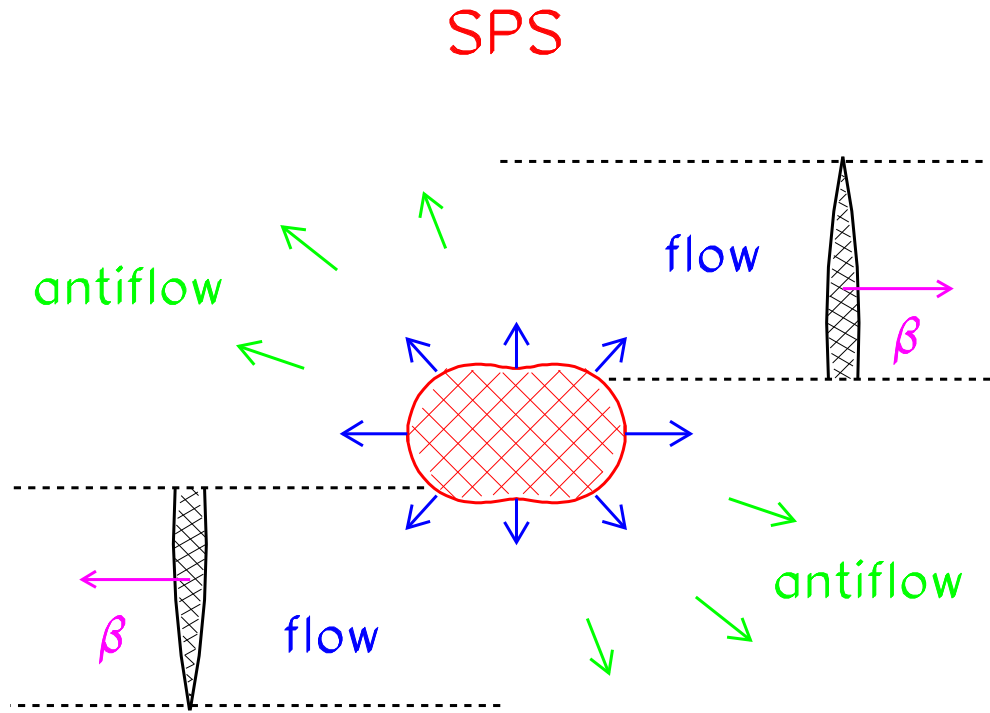


FIG. 10. Formation of the antiflow in the midrapidity range in peripheral collisions at SPS energies. Particles emitted early in the “normal” direction are absorbed by the spectators, while particles emitted in the opposite direction (antiflow) remain unaffected.

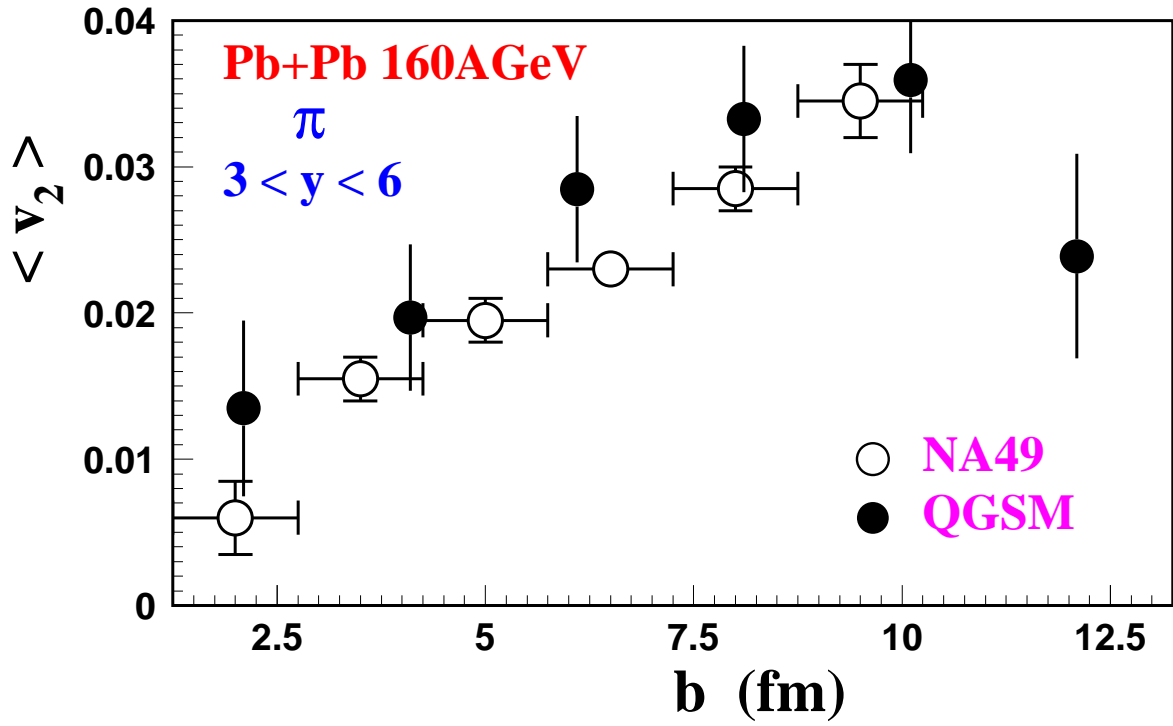


FIG. 11. Elliptic flow of charged pions as function of impact parameter in rapidity range  $3 < y < 6$  in Pb+Pb collisions at 160A GeV. Open circles denote the experimental data from [56], full circles are the model predictions.

TABLES

TABLE I. The slope parameters of the directed flow of nucleons and pions in light and heavy systems in the midrapidity range at the SIS (1A GeV), AGS (11.6A GeV), and SPS (160A GeV) energies.

| System      | Particle | Impact parameter, $\tilde{b} = b/b_{\max}$ |       |       |       |       |       |
|-------------|----------|--|-------|-------|-------|-------|-------|
|             |          | 0.15                                       | 0.30  | 0.45  | 0.60  | 0.75  | 0.90  |
| S+S (SIS)   | N        | 0.12                                       | 0.18  | 0.17  | 0.14  | 0.08  | 0.05  |
|             | $\pi$    | 0.00                                       | -0.02 | -0.03 | -0.03 | -0.02 | -0.01 |
| Au+Au (SIS) | N        | 0.27                                       | 0.37  | 0.37  | 0.33  | 0.26  | 0.22  |
|             | $\pi$    | 0.00                                       | -0.03 | -0.05 | -0.08 | -0.10 | -0.07 |
| S+S (AGS)   | N        | 0.06                                       | 0.10  | 0.13  | 0.13  | -0.02 | -0.05 |
|             | $\pi$    | 0.00                                       | -0.06 | -0.06 | -0.05 | -0.11 | -0.11 |
| Au+Au (AGS) | N        | 0.18                                       | 0.30  | 0.34  | 0.31  | 0.11  | -0.05 |
|             | $\pi$    | -0.07                                      | -0.09 | -0.10 | -0.11 | -0.13 | -0.15 |
| S+S (SPS)   | N        | 0.01                                       | 0.00  | 0.00  | -0.01 | -0.06 | -0.08 |
|             | $\pi$    | 0.00                                       | -0.04 | -0.05 | -0.06 | -0.08 | -0.09 |
| Pb+Pb (SPS) | N        | 0.15                                       | 0.18  | 0.24  | 0.19  | -0.01 | -0.13 |
|             | $\pi$    | -0.03                                      | -0.04 | -0.08 | -0.09 | -0.10 | -0.16 |